plants

MDPI

Article

Effects of Mycotoxin Fumagillin, Mevastatin, Radicicol, and Wortmannin on Photosynthesis of *Chlamydomonas reinhardtii*

Jiale Shi [1,†], Mengyun Jiang [1,†], He Wang [1], Zhi Luo [1], Yanjing Guo [1], Ying Chen [1], Xiaoxi Zhao [1], Sheng Qiang [1], Reto Jörg Strasser [1,2], Hazem M. Kalaji [3] and Shiguo Chen [1,*]

[1] Weed Research Laboratory, Nanjing Agricultural University, Nanjing 210095, China
[2] Bioenergetics Laboratory, University of Geneva, CH-1254 Jussy, Geneva, Switzerland
[3] Department of Plant Physiology, Institute of Biology, Warsaw University of Life Sciences SGGW, Nowoursynowska 159, 02-776 Warsaw, Poland
* Correspondence: chenshg@njau.edu.cn
† These authors contributed equally to this work.

Abstract: Mycotoxins are one of the most important sources for the discovery of new pesticides and drugs because of their chemical structural diversity and fascinating bioactivity as well as unique novel targets. Here, the effects of four mycotoxins, fumagillin, mevastatin, radicicol, and wortmannin, on photosynthesis were investigated to identify their precise sites of action on the photosynthetic apparatus of *Chlamydomonas reinhardtii*. Our results showed that these four mycotoxins have multiple targets, acting mainly on photosystem II (PSII). Their mode of action is similar to that of diuron, inhibiting electron flow beyond the primary quinone electron acceptor (Q_A) by binding to the secondary quinone electron acceptor (Q_B) site of the D1 protein, thereby affecting photosynthesis. The results of PSII oxygen evolution rate and chlorophyll (Chl) *a* fluorescence imaging suggested that fumagillin strongly inhibited overall PSII activity; the other three toxins also exhibited a negative influence at the high concentration. Chl *a* fluorescence kinetics and the JIP test showed that the inhibition of electron transport beyond Q_A was the most significant feature of the four mycotoxins. Fumagillin decreased the rate of O_2 evolution by interrupting electron transfer on the PSII acceptor side, and had multiple negative effects on the primary photochemical reaction and PSII antenna size. Mevastatin caused a decrease in photosynthetic activity, mainly due to the inhibition of electron transport. Both radicicol and wortmannin decreased photosynthetic efficiency, mainly by inhibiting the electron transport efficiency of the PSII acceptor side and the activity of the PSII reaction centers. In addition, radicicol reduced the primary photochemical reaction efficiency and antenna size. The simulated molecular model of the four mycotoxins' binding to *C. reinhardtii* D1 protein indicated that the residue D1-Phe265 is their common site at the Q_B site. This is a novel target site different from those of commercial PSII herbicides. Thus, the interesting effects of the four mycotoxins on PSII suggested that they provide new ideas for the design of novel and efficient herbicide molecules.

Keywords: natural product; photosynthetic inhibitor; mode of action; JIP-test; molecular docking; D1 protein

check for updates

Citation: Shi, J.; Jiang, M.; Wang, H.; Luo, Z.; Guo, Y.; Chen, Y.; Zhao, X.; Qiang, S.; Strasser, R.J.; Kalaji, H.M.; et al. Effects of Mycotoxin Fumagillin, Mevastatin, Radicicol, and Wortmannin on Photosynthesis of *Chlamydomonas reinhardtii*. *Plants* **2023**, *12*, 665. https://doi.org/10.3390/plants12030665

Academic Editor: Maurizio Cocucci

Received: 17 January 2023
Revised: 30 January 2023
Accepted: 31 January 2023
Published: 2 February 2023

1. Introduction

Mycotoxins are low-molecular-weight secondary metabolites naturally produced by fungi. These natural products are one of the most important resource repositories for the discovery of new drugs and pesticides because they possess abundant sources, diverse chemical structures, and wide bioactivity. Generally, they exhibit several phytotoxic, cytotoxic, antimicrobial, and even antitumor activities [1,2]. Some molecular target sites of the known mycotoxins have been described in plants, being involved in amino acid synthesis, energy transfer, PSI electron diverter, PSII electron transport, photosynthetic pigment synthesis, membrane functions and lipid stability, hormonal

regulation, and cell cycle [3]. However, the action targets of many mycotoxins in plant cells remain unknown. Therefore, it is important to clarify the mechanism of action of various mycotoxins in plants. This will provide powerful tools for the study of plant physiological and biochemical mechanisms and will promote the development of new herbicides by directly using mycotoxins or new derivatives synthesized based on these lead templates.

Fumagillin (CAS No. 23110-15-8) is a natural biomolecule originally isolated from *Aspergillus fumigatus*. It is a meroterpenoid produced by the esterification of fumagillol and 2,4,6,8-decatetraenedioic acid (Figure 1A) [4]. Fumagillin can inhibit well-functioning proteins related to cell viability and growth, such as methionine aminopeptidase type 2 enzyme [5]. In agriculture, fumagillin is applied as an antibiotic to prevent microsporidiosis in honeybees and fish [6]. Additionally, Ross et al. [7] showed that fumagillin strongly reduces root development due to the inhibition of methionine aminopeptidase 2 in *Arabidopsis*.

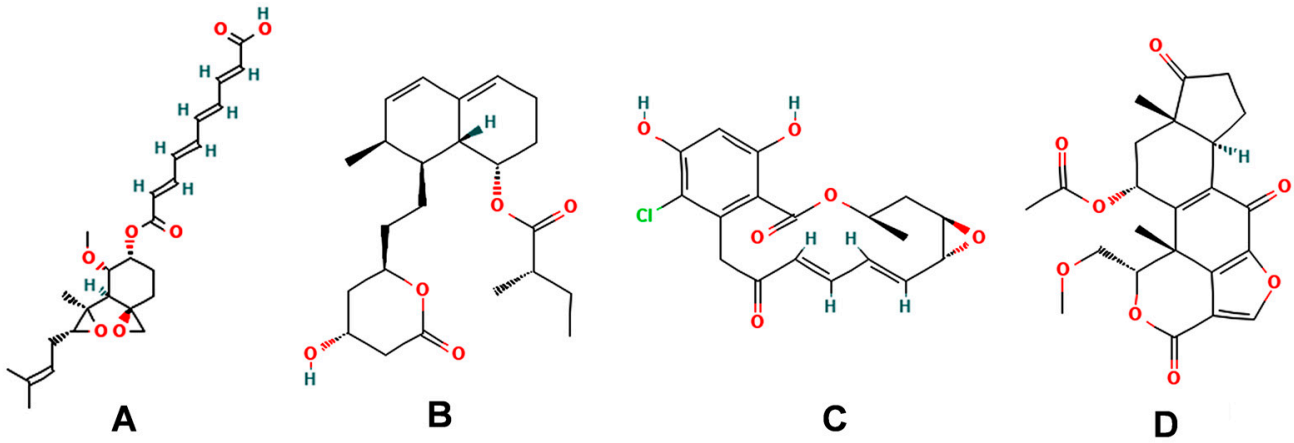

Figure 1. Chemical structure of four mycotoxins: (**A**) fumagillin ($C_{26}H_{34}O_7$, MW: 458.5), (**B**) mevastatin ($C_{23}H_{34}O_5$, MW: 390.5), (**C**) radicicol ($C_{18}H_{17}ClO_6$, MW: 364.8), and (**D**) wortmannin ($C_{23}H_{24}O_8$, MW: 428.4).

Mevastatin (CAS No. 73573-88-3), also called compactin, was first discovered in *Penicillium citinium* [8]. It is a carboxylic ester, consisting of three major functional components, six-membered oxyheterocycle, hexahydronaphthalene, and methylbutyric acid (Figure 1B). Mevastatin is a cholesterol-lowering agent that works by inhibiting 3-hydroxy-3-methylglutaryl-CoA reductase [8]. Thus, it is regarded as a cell apoptosis inducer and has served as a lead compound for the design of new derivatives. Soto et al. [9] suggested that mevastatin can also interrupt the key step of the mevalonate pathway in isoprenoid biosynthesis in plant cytosols.

Radicicol (CAS No. 12772-57-5), known as monorden, was first found in *Monosporium bonorden* [10]. It is also secreted by *Neonectria radicicolas*, *Colletotrichum graminicola*, and other organisms. Radicicol is a 14-membered β-resorcylic acid lactone with a 17R configuration, which is characterized by the resorcyclic acid moiety replaced by a chlorine atom (Figure 1C). It shows significant antibacterial, antifungal, antiviral, anticancer, and antiparasitic activities [11]. Recently, it was demonstrated that radicicol is a specific inhibitor of heat shock protein 90 ATPase activity in *Chlamydomonas reinhardtii* and *Arabidopsis*, reversibly inhibiting the import of abundant preproteins during transmembrane transport [12].

Wortmannin (CAS No. 19545-26-7) is a furanosteroid metabolite derived from the endophytic fungi *Fusarium oxysporum*, *P. wortmannii*, and *P. funiculosum* [13]. It is an organic heteropentacyclic compound containing δ-lactone, acetate ester, and cyclic ketone (Figure 1D). Wortmannin is a dose-dependent inhibitor of phosphatidylinositol 3-kinase and phosphatidylinositol 4-kinase [14]. Therefore, it is an extremely helpful tool in the disruption and identification of vesicular trafficking routes and the definition of endosomal compartments [15]. Wortmannin exhibits excellent cytotoxic activity against human cancer cells [16]. In plant cells, wortmannin interferes with vacuolar transport and causes homotypic fusion and enlargement of multivesicular bodies [17]. It can also accelerate chloroplast division by repressing phosphatidylinositol 4-kinase activity [18].

Photosynthesis is the most important metabolic process in plant growth and development, being very sensitive to changes in environmental conditions. Photosystem II (PSII), as one core of photosynthetic reactions, is a large protein complex located in the thylakoid membranes, including the D1 and D2 proteins as well as several cofactors [19]. Because photosynthesis is specific to green plants, it has attracted much interest in the development of chemical herbicides. Over 50% of the commercial herbicides on the market are photosynthetic inhibitors. Furthermore, fifteen primary targets are located in the photosynthetic apparatus chloroplast among the less than thirty different molecular targets of commercial herbicides [20]. Thus, photosynthesis is often considered a priority when the precise target of a new herbicidal compound needs to be identified in plants. However, up to now, there has been little information on the targets of fumagillin, mevastatin, radicicol, and wortmannin in the photosynthetic apparatus.

In this study, we hypothesized that these four mycotoxins negatively affect photosynthesis, especially PSII activity. To test this hypothesis, the rate of oxygen evolution and chlorophyll (Chl) *a* fluorescence signal of *C. reinhardtii* cells treated with four different mycotoxins were measured to identify their sites of action in photosystems. Because *C. reinhardtii* is one of the most widely used model systems for molecular biological studies of photosystems including extensive characterization of its PSII reaction center, it was used in this study. The model of the interaction between each mycotoxin and the D1 protein of *C. reinhardtii* was also constructed by molecular docking to further confirm their possible binding sites in the D1 protein. Finally, it was demonstrated that four mycotoxins have direct effects on PSII and different binding behavior with the D1 protein from the classical herbicide diuron (DCMU).

2. Results and Discussion

2.1. Effects of Four Mycotoxins on the Oxygen Evolution Rate of PSII

As PSII is an important photosynthetic component that catalyzes light-driven water oxidation, we measured the effect of four mycotoxins on the PSII oxygen evolution rate of *C. reinhardtii* cells. A concentration-dependent decrease in the rate of oxygen evolution of cells exposed to mycotoxin was observed (Figure 2). Fumagillin reduced the rate of oxygen evolution at lower concentrations than the other three mycotoxins. An approximately 61% decrease in the PSII oxygen evolution rate was found in 100 μM fumagillin-treated cells relative to the mock (Figure 2A). However, in the presence of 1000 μM mevastatin, radicicol, or wortmannin, the oxygen evolution rate of *C. reinhardtii* cells was decreased by 51%, 40%, and 45% compared with that of the mock, respectively (Figure 2B,D). All four mycotoxin treatments caused a concentration-dependent decrease in the oxygen evolution rate of PSII, indicating that the photosynthetic activity of PSII was inhibited. In addition, fumagillin was a stronger inhibitor of photosynthetic oxygen evolution than mevastatin, radicicol, and wortmannin. The inactivation of the mycotoxin-induced oxygen evolution mechanism is likely to result in the compromise of its closely related electron transfer efficiency.

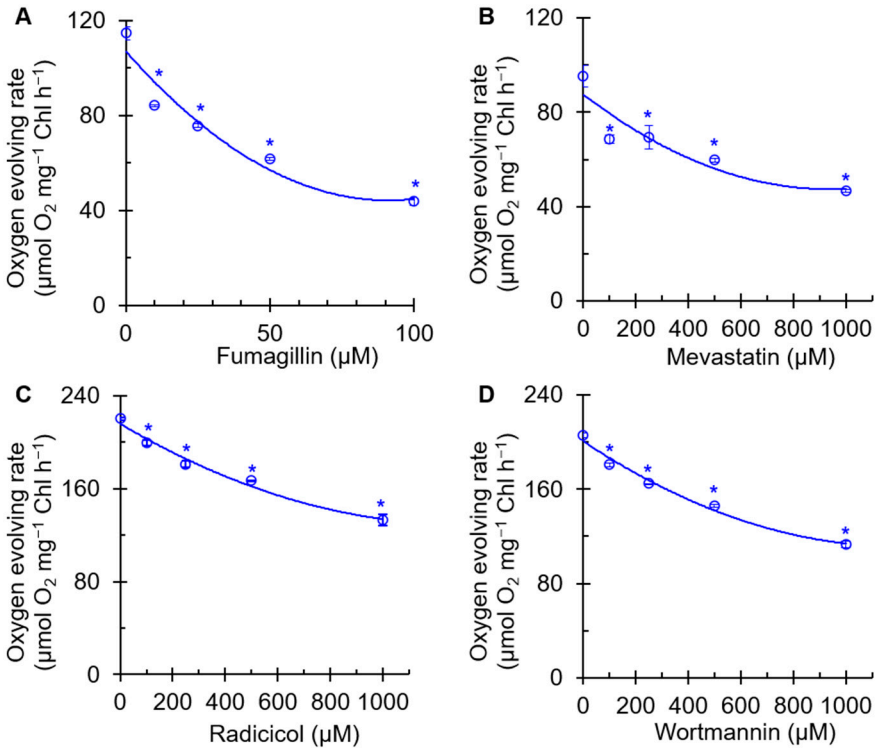

Figure 2. Effects of four mycotoxins, fumagillin (**A**), mevastatin (**B**), radicicol (**C**), and wortmannin (**D**), on oxygen evolving rate of *C. reinhardtii* cells. H_2O and p-phenylenediamine were the electron donor and acceptor, respectively. Data shown are mean values ± SE of three biological replicates. * indicates significance at $p < 0.05$.

2.2. Effects of Four Mycotoxins on Chl *a* Fluorescence Imaging

Chl *a* fluorescence imaging is an expeditious tool used to quickly confirm the photosynthetic damage of green organs, tissues, and even living cells. To further investigate the effect of the four mycotoxins on photosynthetic activity, the Chl fluorescence of mycotoxin-treated *C. reinhardtii* cells was monitored. Based on the results in Figure 2, for subsequent experiments, we chose the concentration of each of the four mycotoxins that had a moderate inhibitory effect on the rate of PSII oxygen precipitation. In Figure 3A, the maximum quantum yields of PSII (F_V/F_M) of fumagillin-, mevastatin-, and radicicol-treated *C. reinhardtii* cell shows a gradual decrease with the color fading from blue to dark green. For wortmannin, no obvious effect on the color-coded images of F_V/F_M was observed at the highest concentration of 600 μM. In the case of the highest concentration of fumagillin (50 μM), mevastatin (200 μM), and radicicol (500 μM), the value of F_V/F_M decreased by approximately 57%, 58%, and 59% compared with that of the mock, respectively. A nearly 5% decrease in the F_V/F_M was observed in the presence of 600 μM wortmannin (Figure 3B). The change in the F_V/F_M was consistent with the change in the fluorescence image presented in Figure 3A. Fumagillin was the most effective in suppressing photosynthetic efficiency, followed by mevastatin and radicicol; the suppressive effect of wortmannin was not reflected by the F_V/F_M parameter. The electron transport rate (ETR) was also measured to evaluate the effect of these mycotoxins on photosynthetic activity (Figure 3C). It could be seen that ETR is a more sensitive fluorescence parameter to these four mycotoxins than F_V/F_M. After *C. reinhardtii* cells were treated with 40 μM fumagillin, 200 μM mevastatin, 400 μM radicicol, or 400 μM wortmannin, the ETR values decreased to zero. The decrease in the ETR value verified our inference that the electron transfer efficiency was influenced by the mycotoxins. These results suggested that these four mycotoxins should inhibit photosynthetic activity; moreover, fumagillin exhibited a stronger inhibitory activity on photosynthetic electron transport than mevastatin, radicicol, and wortmannin.

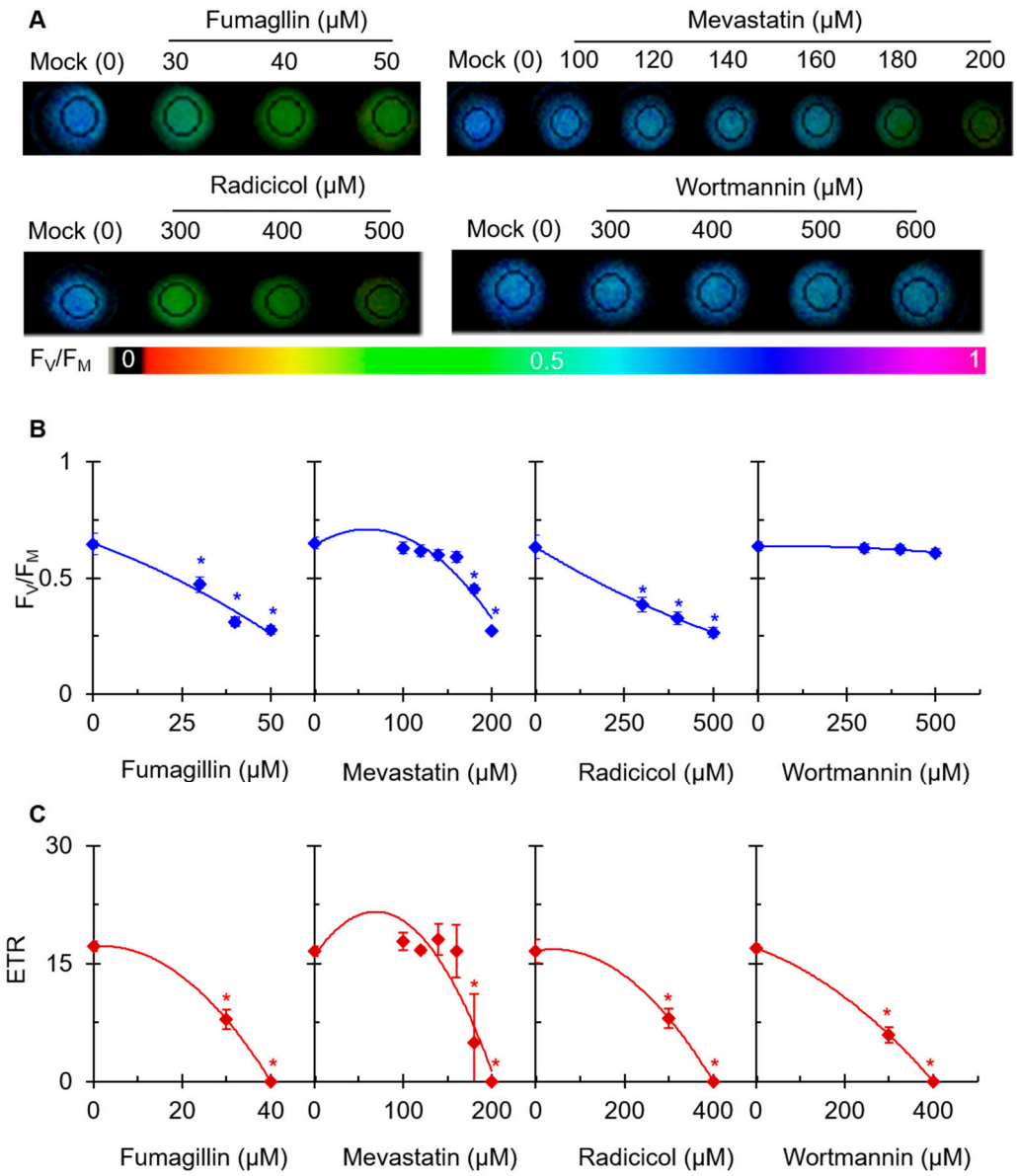

Figure 3. Effects of four mycotoxins on Chl fluorescence of *C. reinhardtii* cells. Cells were incubated for 3 h with different concentrations of fumagillin (30, 40, and 50 μM), mevastatin (100, 120, 140, 160, 180, and 200 μM), radicicol (300, 400, and 500 μM), and wortmannin (300, 400, 500, and 600 μM). (**A**) Color fluorescence images of the maximum quantum yield of PSII (F_V/F_M). (**B**) F_V/F_M value. (**C**) The electron transport rate (ETR). Fluorescence images are indicated by the color code in the order of black (0) through red, orange, yellow, green, blue, and violet to purple (1). Each value is the average ± SE of three biological replicates. * indicates significance at $p < 0.05$.

2.3. Effects of Four Mycotoxins on Chl a Fluorescence Rise Kinetics OJIP

The Chl *a* fluorescence rise kinetics OJIP is an excellent tool to determine the precise effect of different stresses on the photosynthetic apparatus [21]. To investigate the mechanism of action of the four mycotoxins on PSII, the fluorescence rise OJIP curves of *C. reinhardtii* cells were measured after treatment with one of the four mycotoxins for 3 h (Figure 4). It is clear that the raw OJIP curves of DCMU as a positive control and those of each of the mycotoxin-treated cells showed a visible change compared with the typical polyphasic OJIP curve of the mock. Under 50 μM DCMU treatment, the J step quickly increased to the equal P level (F_M), which is the main change in the OJIP curve relative to the mock. Radicicol and wortmannin at 500 μM, as with DCMU, caused a remarkably fast rise in the

J step. Interestingly, the IP phase of the OJIP curve of DCMU- and wortmannin-treated cells disappeared entirely, but still remained in the radicicol-treated cells (Figure 4A). Meanwhile, just a slight increase in the J-step level of the OJIP curve could be observed in 50 μM fumagillin- or 200 μM mevastatin-treated cells. Because a rise in the J step contributes to the large accumulation of reduced primary quinone electron acceptor (Q_A^-) in PSII reaction centers (RCs), resulting from the interruption of electron flow beyond Q_A at the PSII acceptor side [21,22], it was suggested that electron transferring beyond Q_A at the acceptor side of PSII was strongly inhibited by radicicol and wortmannin. This agreed with the ETR results (Figure 3C). However, 50 μM fumagillin and 200 μM mevastatin treatments led to a slight decrease in PSII electron flow beyond Q_A. In addition, a distinct lift in the O step in fumagillin- and radicicol-treated cells, and an obvious decrease in the P-step level in radicicol-treated cells, were observed (Figure 4A).

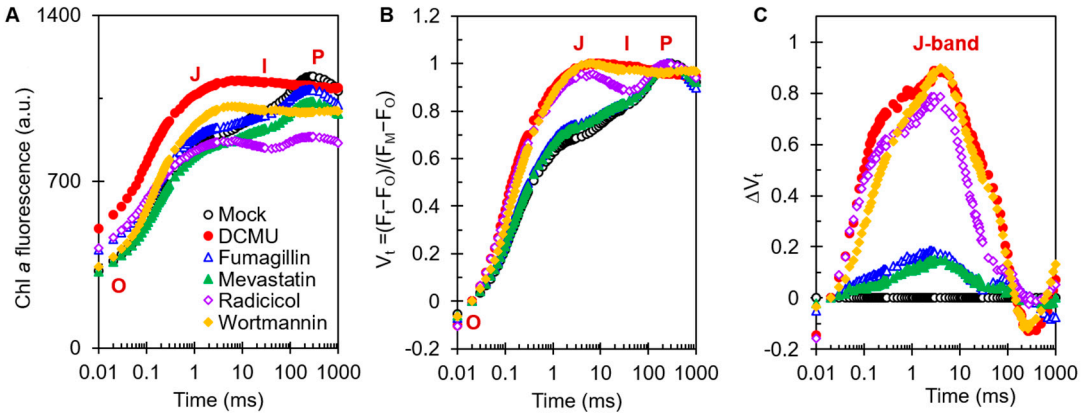

Figure 4. Effects of four mycotoxins and DCMU on Chl *a* fluorescence rise kinetics of *C. reinhardtii* cells. Cells after 3 h of treatment with 0.1 % DMSO (mock), 50 μM DCMU, 50 μM fumagillin, 200 μM mevastatin, 500 μM radicicol, or 500 μM wortmannin. (**A**) Raw fluorescence rise OJIP curves of mock-, DCMU-, fumagillin-, mevastatin-, radicicol-, and wortmannin-treated *C. reinhardtii* cells. (**B**) Chl *a* fluorescence rise kinetics normalized by F_O and F_M as $V_t = (F_t - F_O)/(F_M - F_O)$ versus logarithmic timescale. (**C**) The difference kinetics $\Delta V_t = V_{t(treatment)} - V_{t(mock)}$ versus logarithmic timescale. Each curve is the average of 30 measurements.

To visualize the features that were hidden behind the raw fluorescence rise kinetics OJIP curves, the OJIP curves of mock-, DCMU-, and mycotoxins-treated cells were double -normalized between F_O and F_M, which is expressed as the relative variable fluorescence $V_t = (F_t - F_O)/(F_M - F_O)$ (Figure 4B) and $\Delta V_t = V_{t(treatment)} - V_{t(mock)}$ (Figure 4C) on a logarithmic time scale. It was revealed that the biggest change in the OJIP curves of the mycotoxins-treated cells was a noticeable increase in the J band, which was similar to the effect of DCMU. So, the dominant effect of the four mycotoxins on the photosynthesis of *C. reinhardtii* is blocking PSII electron transfer beyond Q_A at the acceptor side.

The differences in the curve changes caused by different mycotoxins are also very interesting. For fumagillin, the O step of the treated cells was slightly elevated, which was similar to the results of DCMU treatment. A rise in the O step represents an increase in the initial yield of fluorescence, which may be the result of the partial or complete inactivity of the oxygen-evolving complexes (OECs) of *C. reinhardtii* cells [23,24]. For radicicol, the O step was significantly higher, whereas the P step was significantly lower. The decrease in the P step is due to fluorescence quenching caused by the interaction between oxidized plastoquinone (PQ) molecules and the PSII antenna [24]. For mevastatin, only a slight increase in the J peak and a slight decrease in the IP phase were observed (Figure 4A). It is normally considered that the I step and IP phase represent the redox state of PQ and the redox state of the terminal receptor on the electron acceptor side of PSI, respectively [21,25]. This suggested that the inhibition of photosynthetic efficiency by mevastatin was mainly attributed to the inhibition of PSII electron transport beyond Q_A, and the redox status of

downstream acceptors was consequently affected. For 500 μM wortmannin treatment, the J peak sharply increased and was similar to the J-step increase for radicicol at the same concentration (Figure 4B,C), indicating that wortmannin and radicicol had similar abilities to inhibit electron transfer, which supports the results in Figure 3C.

2.4. Effects of Four Mycotoxins on the Selected JIP Test Parameters

The JIP test parameters give adequate information about the structure, conformation, and function of the photosynthetic apparatus, especially PSII [21]. Some selected JIP test parameters are presented to further confirm the effect of the four mycotoxins on PSII of *C. reinhardtii* (Figure 5). Both fumagillin and radicicol increased the F_O. Only radicicol clearly decreased the F_M value (Figure 5A). Fumagillin, radicicol, and wortmannin caused a decrease in the F_V/F_M which was related to the change in F_O and/or F_M. Mevastatin had nearly no effect on F_O, F_M, or F_V/F_M. F_O and F_M are the results of O-step and P-step quantization in the OJIP curve, respectively. The results suggested that fumagillin and radicicol might inhibit the activity of OECs in *C. reinhardtii* cells (increase in F_O); radicicol might lead to oxidation of the PQ pool or disruption of PSII antennae (decrease in F_M); and fumagillin, radicicol, and wortmannin have different degrees of inhibition of the quantum efficiency of light energy transfer in PSII (decrease in F_V/F_M). In addition, 200 μM mevastatin showed insensitivity to F_V/F_M.

All four mycotoxins significantly changed the relative variable fluorescence at the J step (V_J) and ΔV_J (Figure 5B). The changes in these technical fluorescence parameters are perfectly agreement with the results in Figure 4. In the DCMU-treated samples, V_J and ΔV_J significantly increased due to the large accumulation of Q_A^- in PSII RCs, resulting in the blocking of electron flow beyond Q_A [21]. For the treatment with fumagillin (50 μM) or mevastatin (200 μM), the ΔV_J values were significantly lower than those of the DCMU (50 μM) treatment. In contrast, the ΔV_J values under radicicol (500 μM) or wortmannin (500 μM) treatment were close to those of the DCMU (50 μM) treatment. Thus, the four mycotoxins showed similarities to DCMU in the inhibition pattern of electron transport, but the inhibition effects were significantly different. The inhibition by the four mycotoxins was significantly weaker than that of DCMU, and the inhibition of wortmannin was slightly stronger than that of radicicol. Moreover, radicicol and wortmannin showed an increase in relative variable fluorescence at the I step (V_I). The values of both fluorescence parameters V_J and V_I are considered to correlate with the state of electron transport on the PSII acceptor side [21,26], particularly the increases of V_J values indicated that the four mycotoxins blocked PSII electron transport beyond Q_A.

To further verify the inhibition of electron transport from Q_A to the secondary quinone electron acceptor (Q_B) by the four mycotoxins, the parameters φ_{Eo}, ψ_{Eo}, and ET_0/RC were analyzed (Figure 5C). φ_{Eo} expresses the quantum yield for electron transport [26]. ψ_{Eo} is the probability that an electron moves further than Q_A^- into the electron transport chain [27]. ET_0/RC reflects the electron transport per RC [26]. In the presence of the four mycotoxins, the values of φ_{Eo}, ψ_{Eo}, and ET_0/RC were all significantly decreased relative to mock, indicating that the four mycotoxins did interrupt PSII electron transfer from Q_A to Q_B.

Because of the negative effect of the four mycotoxins on PSII electron transport, it as expected that the PSII RCs' activity might have been inhibited as a result. The values of S_m/t_{FM} in radicicol- and wortmannin-treated cells were clearly lower than that of the mock (Figure 5D). The parameter S_m denotes the normalized total complementary region above the O-J-I-P transient, reflecting multiple-turnover Q_A reduction events [27]. The parameter t_{FM} means the time to reach F_M [26]. The S_m/t_{FM} ratio represents a measure of the average redox state of Q_A^-/Q_A from zero to t_{FM} time and expresses the average fraction of open RCs [28]. However, the values of S_m/t_{FM} did not significantly change in fumagillin- and mevastatin-treated cells, indicating that fumagillin (50 μM) and mevastatin (200 μM) probably do not affect the activity of PSII RCs. Another fluorescence parameter, R_J, explains the inactivation of PSII RCs. It is generally considered that R_J reflects the

number of PSII RCs with the Q_B site filled populated by PSII inhibitors [27]. For fumagillin- (50 μM), mevastatin- (200 μM), radicicol- (500 μM), and wortmannin- (500 μM) treated cells, the values of R_J increased by 16%, 13%, 74%, and 84% relative to the mock, respectively (Figure 5D). This suggested that the four mycotoxins inhibited PSII electron transfer activity due to their filling in the Q_B site. Thus, we suggest that the inactivation of the PSII RCs caused by radicicol and wortmannin is attributable to the inhibition of PSII electron transport. The insignificant effect of fumagillin and mevastatin on PSII RCs may be owing to the insufficient number of PSII RCs at the Q_B site filled by them and thus the insufficient inhibition of electron transfer.

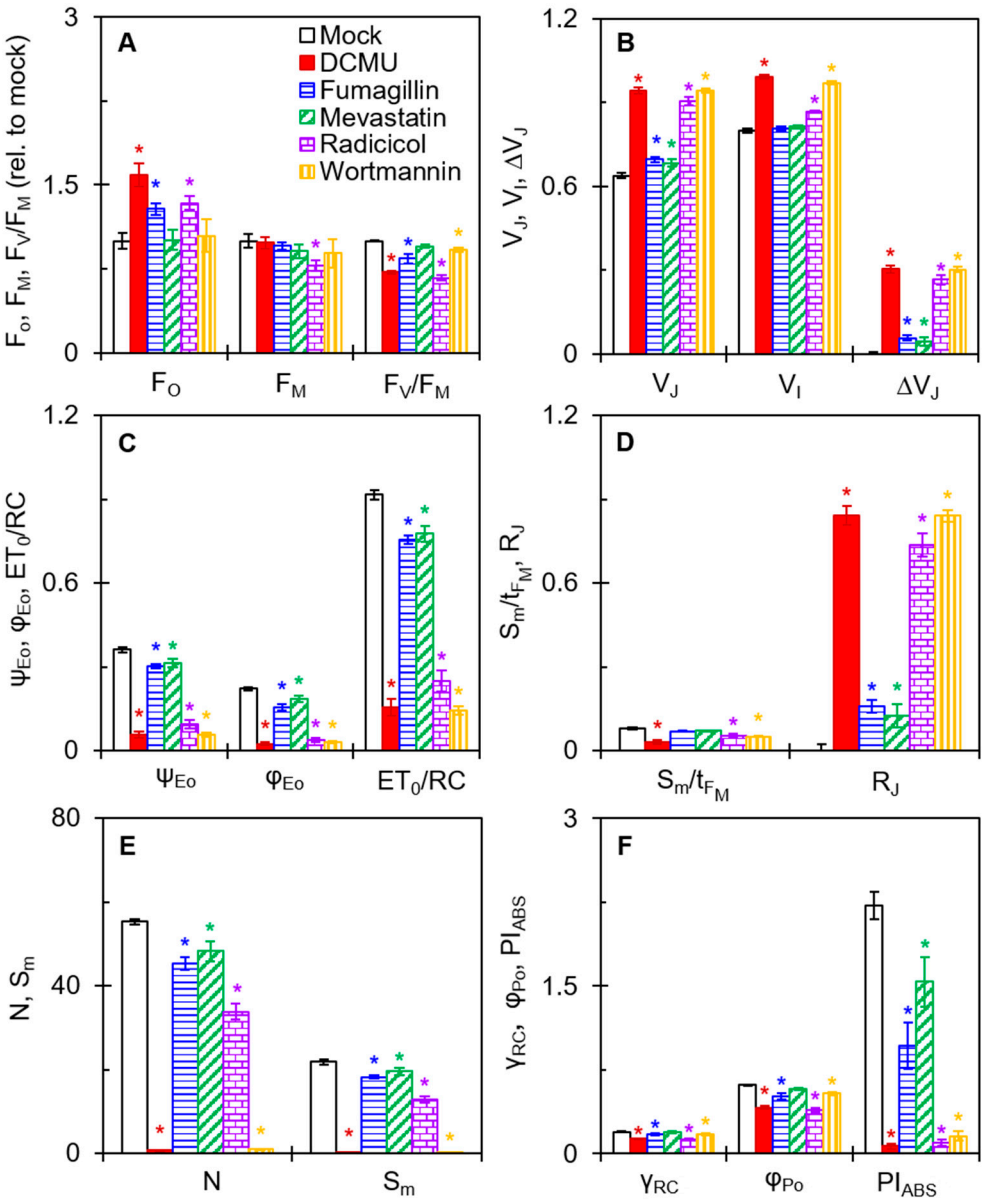

Figure 5. Effects of four mycotoxins on the selected JIP test parameters of *C. reinhardtii* cells. (**A**) The relative values of F_O, F_M, and F_V/F_M after mycotoxins treatment compared with mock. (**B**) The values of V_J, V_I, and ΔV_J. (**C**) The values of ψ_{Eo}, φ_{Eo}, and ET_0/RC. (**D**) The values of S_m/t_{FM} and R_J. (**E**) The values of N and S_m. (**F**) The values of γ_{RC}, φ_{Po}, and PI_{ABS}. Each parameter is the average of 30 measurements. * indicates significance at $p < 0.05$.

The values of the N and S_m parameters further support the above results (Figure 5E). The turnover number N represents the number of Q_A reduction events between time zero and t_{FM} [26]. Compared with the mock, the values of N and S_m slightly decreased for fumagillin and mevastatin treatment and sharply decreased for radicicol and wortmannin treatment. Wortmannin treatment especially decreased the N and S_m values almost to zero. The changes in these JIP test parameters with wortmannin-treated cells were much stronger than those of the other mycotoxins, which as almost equivalent to that of DCMU (Figure 5C,E). A decrease in S_m represents a reduction in the total electron-accepting capacity of leaves, which measures the electron transporter pool between PSII and PSI acceptors [29,30]. Wortmannin strongly blocked electron transport and thus caused a severe inactivation of PSII RCs. So far, there are many reports of the inactivation of PSII RCs caused by natural products with PSII inhibitory activity. It was reported that fischerellin A [31] significantly increased the J step in cyanobacteria, green algae, and pea leaves, inhibiting electron transport and leading to the inactivation of PSII RCs. Tenuazonic acid [27] and patulin [32] have been found to inhibit electron flow from Q_A to Q_B in higher plants as well, thereby inactivating PSII RCs. Previous studies have shown that a decrease in the number of active PSII RCs causes an increase in non-Q_A-reducing centers [21,27]. The non-Q_A-reducing centers, namely the heat sink centers, eliminate the redundant excitation energy mainly by increasing thermal dissipation, leading to harmful reactive oxygen species (ROS) generation.

PI_{ABS} is the most sensitive JIP test parameter, which is used to assess the photosynthetic performance indexes of samples [27]. When *C. reinhardtii* cells were incubated with fumagillin, mevastatin, radicicol, or wortmannin, the values of PI_{ABS} decreased by 61%, 31%, 95%, and 93% compared with that of the mock, respectively (Figure 5F). Significant changes in parameter PI_{ABS} are closely related to the antenna size (γ_{RC}), the maximum quantum yield of primary photochemistry (φ_{Po}), and the probability of electrons on the reduced Q_A. further entering the electron transfer chain [21,27]. The treatment with fumagillin and radicicol reduced γ_{RC} by 15% and 35%, respectively. The φ_{Po} of *C. reinhardtii* cells decreased by 18%, 37%, and 13%, respectively, under fumagillin, radicicol, and wortmannin treatment. Mevastatin showed no significant effect on the parameters γ_{RC} and φ_{Po}, and wortmannin showed no significant effect on φ_{Po}. The ψ_{Eo} decreased with fumagillin, mevastatin, radicicol, and wortmannin treatment by 17%, 11%, 72%, and 83%, respectively, as shown in Figure 5C. For fumagillin, the decrease in PI_{ABS} is related to the changes in the parameters γ_{RC}, φ_{Po}, and ψ_{Eo}. In other words, fumagillin harmed the antenna size, primary photochemical reaction, and redox reaction after Q_A, which together significantly reduced the overall photosynthetic activity of PSII. For mevastatin and wortmannin, the decrease in PI_{ABS} was only associated with a significant decrease in the parameter ψ_{Eo}. The main mechanism of action of mevastatin and wortmannin is the inhibition of electron transport beyond the Q_A. As for radicicol, γ_{RC}, φ_{Po}, and ψ_{Eo} were significantly affected, but ψ_{Eo} was clearly the dominant factor. This suggested that the main factor for the decrease of PI_{ABS} by radicicol as the reduced efficiency of movement in the redox reaction of the electron transport chain. The inhibition of the flow of PSII electrons from Q_A to Q_B remained a common feature of the mechanism of action of the four mycotoxins.

To summarize, we found that the common and dominant mechanism of action of the four mycotoxins in inhibiting photosynthetic activity was to block electron transfer on the acceptor side of PSII by occupying the Q_B site. This further resulted in different degrees of reduction in the number of active PSII RCs and the overall photosynthetic activity of PSII. It has been widely reported that the interruption of electron transport has some negative effects on photosynthesis. For example, reduced electron transport capacity limits the synthesis of ATP and thus inhibits the regeneration of RuBP and the assimilation of CO_2 [33,34]; the blockage of electron flow leads to an increase in the number of escaped electrons and thus increases the production of dangerous ROS [35]. In addition, we noticed that the multiple negative effects of fumagillin and radicicol on OEC activity, primary photochemical reaction, and antenna size also affected photosynthesis.

2.5. Modeling of Four Mycotoxins' Binding Niche at the Q_B-Site of the D1 Protein

PSII is an important part of photosynthesis, which provides the initial charge separation to generate high-energy electrons for photosynthetic electron transport. The PSII RC core consists of two highly hydrophobic proteins, D1 and D2, which embed most of the redox active components involved in photosynthetic electron transfer through PSII [19]. The Q_B niche on the D1 subunit is a binding target for many known PSII inhibitor herbicides [36], which compete with Q_B for the Q_B binding site during electron transport, ultimately leading to plant death [37]. The Q_B-binding pocket is a cavity lined with hydrophobic residues located in the connecting loop between the fourth and fifth transmembrane helices of the D1 protein, which consists of at least 65 amino acids spanning from Phe211 to Leu275 [19]. All these amino acids are highly conserved in representatives of cyanobacteria, algae, and plants, implying that the Q_B site is also conserved in oxygenic photosynthetic organisms [38].

To further confirm the binding site of the four mycotoxins in the D1 protein, the crystal structure of the *C. reinhardtii* D1 protein (Protein Data Bank (PDB): 6KAC) was selected to model the position of the four mycotoxins in the Q_B site with Discovery Studio (version 2016, BIOVIA, San Diego, CA, USA) (Figures 6 and 7 and Table 1). The proposed molecular model showed that the D1-Phe265 residue was the common binding site of the four mycotoxins in the Q_B site, which formed a hydrogen bond with the oxygen atom of four mycotoxins. Interestingly, the hydrogen bond donor of mevastatin was carbonyl oxygen (CO) of the D1-Phe265 residue instead of amino hydrogen (NH). The simulated modeling distances of the hydrogen bonds of fumagillin, mevastatin, radicicol, and wortmannin were 2.53 Å, 2.67 Å, 2.52 Å and 2.39 Å, respectively. The four mycotoxins also established several hydrophobic, Pi-stacking, and hydrogen-bonding interactions with active site residues, as detailed in Table 1. Hydrogen bonding is considered to play a crucial role in the stability of a structure. Van der Waals, hydrophobic, and Pi-stacking interactions are also involved in the stabilization of mycotoxin binding to the Q_B site. Compared with the other models, the fumagillin model showed the largest number of bonding interactions with D1. Our previous experimental results also showed that fumagillin had the strongest inhibitory effect on PSII, with the highest affinity in vitro (Figures 2 and 3C). These results suggest that fumagillin may have the highest affinity for the Q_B site of the D1 protein among the four mycotoxins.

The standard model of the classical PSII herbicide DCMU docking to the Q_B binding site was established to verify the reliability of the binding model. Our model showed that the possible hydrogen binding interaction for DCMU and D1 was formed between the N7 of DCMU and D1-Ser264 Oγ with a 2.37 Å bound distance (Figure 6E and Table 1). The DCMU was completely nestled in the cavity formed by the Q_B binding pocket, forming non polar interactions with D1-Leu218, D1-His252, and D1-Leu271 (Figure 7E). Early crystallographic investigations of PSII and studies with resistant mutants support that D1-Ser264 plays a key role in DCMU binding to the Q_B site [37,39,40]. Previous studies showed that the amide hydrogen of DCMU may form a hydrogen bond with the hydroxyl oxygen of D1-Ser264. Another weak hydrogen bridge is formed between the carbon group of DCMU and the side chain of D1-His215 [19]. In the herbicide-resistant mutant experiment of *C. reinhardtii*, the residue Ser264 mutation in the D1 protein conferred DCMU resistance [39]. Our modeling is in agreement with the existing data, with high reliability and accuracy.

The surface representations of the four mycotoxins bound to the Q_B site showed their positions in the binding pocket (Figure 7). The short alkyl side chain of fumagillin entered inside the cavity, and its long unsaturated carboxyl side chain and cyclohexane ring were partly exposed outside the cavity (Figure 7A). The six-membered oxygen-containing hetero ring of mevastatin entered the Q_B binding pocket; other parts lay along the wall of the cavity (Figure 7B). For radicicol, the fifteen-membered hetero ring entered the Q_B binding pocket, except for the benzene ring (Figure 7C). The results of the docking model suggested that the four mycotoxins show binding affinity for binding the Q_B site. However, DCMU totally enters the cavity formed by the Q_B binding pocket (Figure 7E). This may be the

reason why the inhibitory activity of the four mycotoxins against PSII was weaker than that of DCMU.

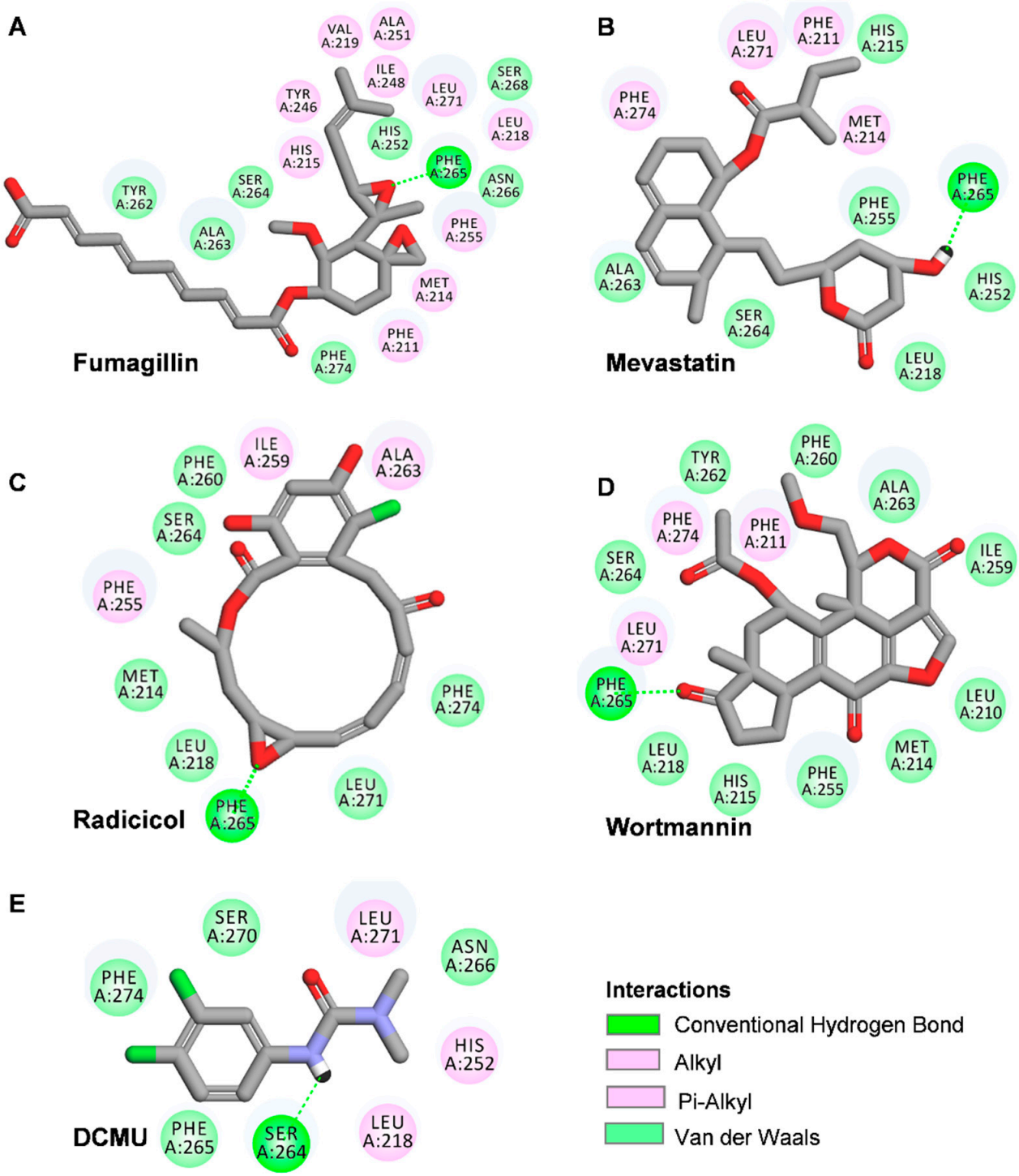

Figure 6. Hydrogen-bonding interactions for fumagillin (**A**), mevastatin (**B**), radicicol (**C**), wortmannin (**D**). and DCMU (**E**) in the Q_B binding site of D1 protein of *C. reinhardtii* (6KAC). Here, carbon atoms are shown in grey, nitrogen atoms in blue, oxygen in red, chlorine atoms in green, and hydrogen atoms in white. Possible hydrogen bonds are indicated by a dashed line.

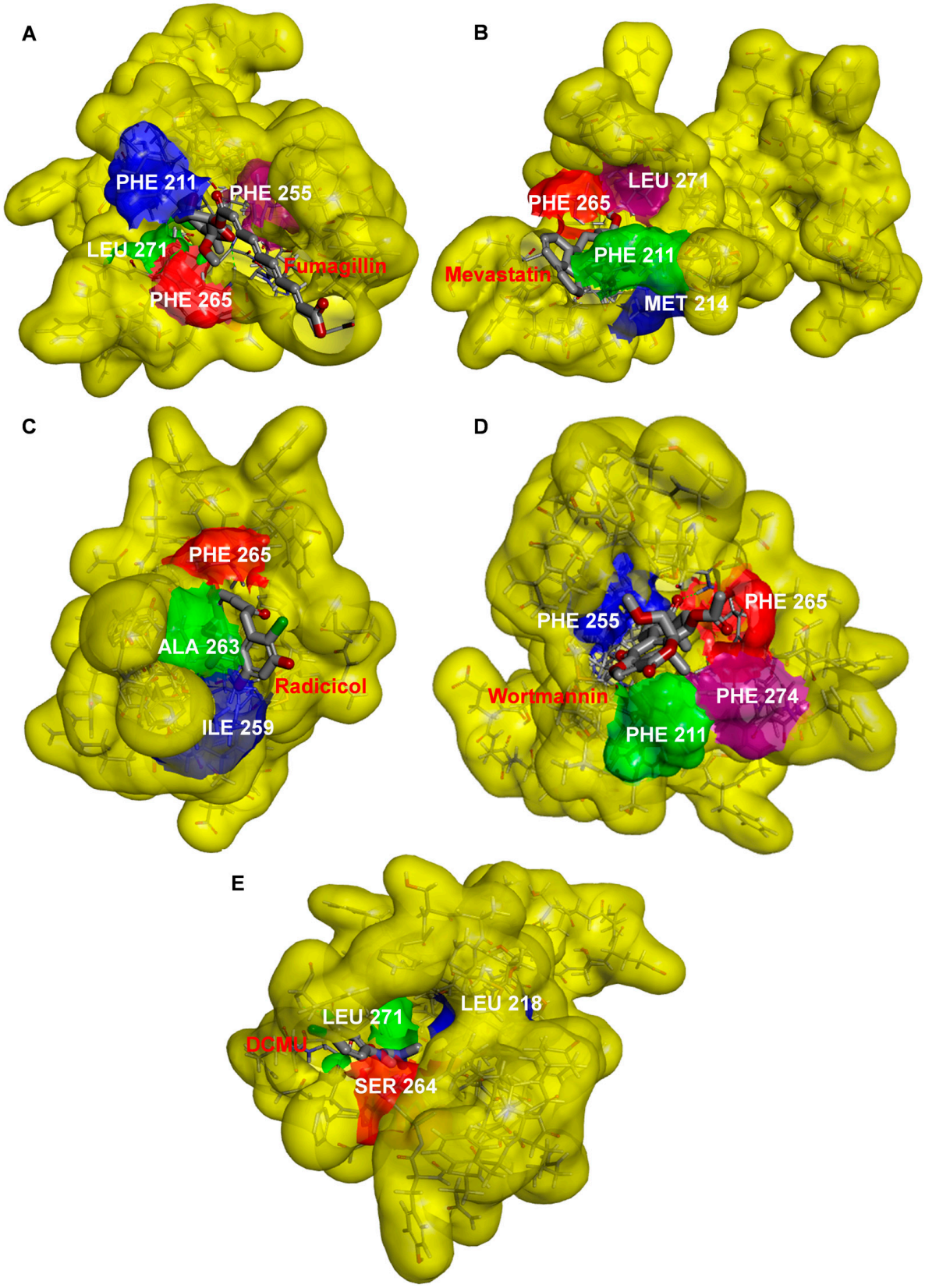

Figure 7. Docked poses of fumagillin (**A**), mevastatin (**B**), radicicol (**C**), wortmannin (**D**), and DCMU (**E**) inside the Q_B binding site of D1 protein of *C. reinhardtii* (6KAC).

It is well known that the negative effects of weed resistance are usually associated with the long-term and large-scale use of conventional herbicides [41]. PSII inhibitors have been classified as the urea/triazine type or phenol type according to their structural characteristics and modes of inhibition, both of which have their characteristic orientation in D1 proteins. Previous studies have suggested that urea/triazine herbicides prefer to orient toward Ser264, while the preferential binding orientation of phenol herbicides is His215 [36,37]. Due to the proliferation of resistant weeds, the development of herbicides with new target sites has become more urgently required. Natural herbicides have received widespread attention because of their novel structures, unique targets, and environmental friendliness. Some natural PSII inhibitors are tenuazonic acid and patulin, which have unique binding orientation at the Q_B site. The docking model of tenuazonic acid to *Arabidopsis* D1 protein showed that tenuazonic acid is preferentially oriented to D1-Gly256 by a hydrogen bond [42]. By docking patulin to the *Ageratina adenophora* D1 protein, patulin was found to bind to the Q_B site by forming a hydrogen bond with the His252 residue in the D1 protein [32]. Based on molecular docking models of four mycotoxin bounding to *C. reinhardtii* D1 proteins, we concluded that residue Phe265 is the key residue for the interaction of the four mycotoxins with D1, which is clearly different from the key active site of commercial herbicides and reported natural PSII inhibitors. Therefore, these mycotoxins cannot be directly applied as herbicides but may provide ideas for the development and synthesis of novel herbicides in the future. However, their binding environment needs to be further verified by crystallographic data and mutant experiments.

Table 1. Possible binding interactions for DCMU, fumagillin (Fum), mevastatin (Mev), radicicol (Rad), and wortmannin (Wor) to the D1 protein of *C. reinhardtii.*

Compound	Molecular Formula	Chemical Structure	Donor	Acceptor	Interactions	Bound Distance (Å)
DCMU	$C_9H_{10}Cl_2N_2O$	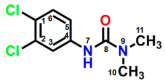	D1-Leu 218	DCMU C10	Alkyl Hydrophobic	3.15
			D1-His 252	DCMU C11	Alkyl Hydrophobic	3.22
			D1-Ser 264 Oγ	DCMU NH	Hydrogen Bond	2.37
			D1-Leu 271	DCMU C11	Alkyl Hydrophobic	3.17
Fumagillin	$C_{26}H_{34}O_7$	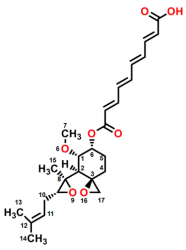	D1-Phe 211	Fum C17	Pi-Hydrophobic	3.52
			D1-Met 214	Fum C17	Alkyl Hydrophobic	3.48
			D1-His 215	Fum C7	Alkyl Hydrophobic	3.63
			D1-Leu 218	Fum C13	Alkyl Hydrophobic	3.67
			D1-Val 219	Fum C13	Alkyl Hydrophobic	3.18
			D1-Tyr 246	Fum C13	Alkyl Hydrophobic	3.23
			D1-Ile 248	Fum C12	Alkyl Hydrophobic	3.20
			D1-Ala 251	Fum C12	Alkyl Hydrophobic	3.49
			D1-Phe 255	Fum C15	Pi Hydrophobic	3.64
			D1-Phe 265 NH	Fum O9	Hydrogen Bond	2.53
			D1-Leu 271	Fum C12	Alkyl Hydrophobic	3.36
Mevastatin	$C_{23}H_{34}O_5$	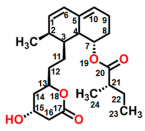	D1-Phe 211	Mev C23	Pi Hydrophobic	3.21
			D1- Met 214	Mev C9	Alkyl Hydrophobic	3.18
			D1-Phe 265 CO	Mev C15-OH	Hydrogen Bond	2.67
			D1-Leu 271	Mev C23	Alkyl Hydrophobic	3.55
			D1-Phe 274	Mev C24	Pi Hydrophobic	3.46
Radicicol	$C_{18}H_{17}ClO_6$	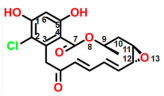	D1-Phe 255	Rad C9-CH_3	Pi Hydrophobic	3.31
			D1-Ile 259	Rad Ph	Pi Hydrophobic	3.64
			D1-Ala 263	Rad Ph	Pi Hydrophobic	3.57
			D1-Phe 265 NH	Rad O13	Hydrogen Bond	2.52
Wortmannin	$C_{23}H_{24}O_8$	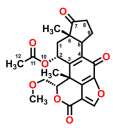	D1-Phe 211	Wor C12	Pi Hydrophobic	3.51
			D1-Phe 265 NH	Wor O7	Hydrogen Bond	2.39
			D1-Leu 271	Wor C6-CH_3	Alkyl Hydrophobic	3.28
			D1-Phe 274	Wor C12	Pi Hydrophobic	3.37

3. Materials and Methods

3.1. Plant Materials and Chemicals

The *C. reinhardtii* wild-type strain was obtained from the Freshwater Algae Culture Collection at the Institute of Hydrobiology (FACHB-collection, Chinese Academy of Science, Wuhan, China). *C. reinhardtii* cells were cultured in liquid tris-acetate phosphate media (TAP) under 100 μmol (photons) m^{-2} s^{-1} white light with a 12 h photoperiod at 25 °C. Three-day-old cells in the logarithmic growth phase were collected for further experiments [26].

Fumagillin, mevastatin, radicicol, wortmannin, 3-(3,4-dichlorophenyl)-1,1-dimethylurea (DCMU), dimethyl sulfoxide (DMSO), and other chemical agents were purchased from Sigma-Aldrich (Shanghai, China). Four mycotoxins and DCMU stock solutions were dissolved in 100% DMSO and further diluted with sterile water. The final concentration of DMSO in the working solutions of all chemical agents was less than 1% (*v*/*v*).

3.2. Measurement of PSII Oxygen Evolution Rate

The rate of oxygen evolution of PSII was measured using a Clark-type Oxygen Electrode (Hansatech Instruments Ltd., King's Lynn, UK) according to the method of Guo et al. [43]. After *C. reinhardtii* cells were collected, they were washed and resuspended in buffer A containing 20 mM HEPES (pH 7.5), 350 mM sucrose, and 2.0 mM $MgCl_2$ with an A_{750} value of 0.65. Each mycotoxin was added into 2 mL cell suspensions with the indicated concentrations. The samples were incubated for 3 h in the dark at 25 °C. Subsequently, treated cells containing 45 μg of chlorophylls were added into 2 mL of PSII reaction medium (50 mM HEPES-KOH at pH 7.6, 4 mM $K_3Fe(CN)_6$, 5mM NH_4Cl, and 1 mM p-phenylenediamine). The oxygen evolution rate was determined and recorded during the first three minutes after samples were illuminated with 400 μmol (photons) m^{-2} s^{-1} red light.

3.3. Chl a Fluorescence Imaging

Chl *a* fluorescence imaging, F_V/F_M, and the ETR of dark-adapted samples were measured using a pulse-modulated Imaging-PAM M-series fluorometer (MAXI-version, Heinz Walz GmbH, Effeltrich, Germany) [43]. Cells were resuspended with buffer A. We added 200 μL of cell suspension with the indicated concentrations of fumagillin, mevastatin, radicicol, wortmannin, or 1% DMSO (mock) to a 96-well black microtiter plate. The cell suspensions were incubated for 2.5 h under light (100 μmol m^{-2} s^{-1}) at 25 °C. Then, samples were dark-adapted for 30 min under the imaging system camera. For monitoring fluorescence imaging, the measuring light, actinic light, and saturation pulse light were set to 0.25, 110, and 6000 μmol (photons) m^{-2} s^{-1}, respectively.

3.4. Chl a Fluorescence Rise Kinetics OJIP and JIP-Test

The Chl *a* fluorescence rise kinetics OJIP were measured with a Plant Efficiency Analyzer (Hansatech Instruments Ltd., King's Lynn, UK) [27]. We incubated 1 mL of cell suspension in buffer A with 1% DMSO (mock), 50 μM DCMU, 50 μM fumagillin, 200 μM mevastatin, 500 μM radicicol, or 500 μM wortmannin for 2.5 h under 100 (photons) μmol m^{-2} s^{-1} white light at 25 °C. The cells were collected and resuspended in 20 μL of buffer A. After 30 min dark adaptation, 20 μL of the sample was filtered onto a glass microfiber filter (diameter 25 mm, GF/C, Whatman, Kent, UK) and clamped with a leaf clip. Samples were illuminated with continuous red light (650 nm peak wavelength, 3500 μmol (photons) m^{-2} s^{-1} maximum light intensity). The raw data were transferred to a computer using Handy PEA software (version 1.30, Hansatech Instruments Ltd., Norfolk, UK). The experiment was repeated three times with at least 15 repetitions. The detailed parameters and definitions re listed in Table 2, according to Strasser et al. [21] and Chen et al. [27].

Table 2. Formulae and explanation of technical data of the OJIP curves and the selected JIP test parameters used in this study.

Technical Fluorescence Parameter	
F_t	fluorescence at time t after onset of actinic illumination
$F_O \cong F_{20\mu s}$	minimal fluorescence, when all PSII RCs are open
$F_K \equiv F_{300\mu s}$	fluorescence intensity at the K step (300 μs) of OJIP
$F_J \equiv F_{2ms}$	fluorescence intensity at the J step (2 ms) of OJIP
$F_I \equiv F_{30ms}$	fluorescence intensity at the I step (30 ms) of OJIP
F_P (=F_M)	maximal recorded fluorescence intensity, at the peak P of OJIP
$F_v \equiv F_t - F_O$	variable fluorescence at time t
$F_V \equiv F_M - F_O$	maximal variable fluorescence
t_{FM}	time (in ms) to reach the maximal fluorescence intensity F_M
Area	total complementary area between the fluorescence induction curve and F = F_M
$V_t \equiv (F_t - F_O)/(F_M - F_O)$	relative variable fluorescence at time t
$V_J = (F_J - F_O)/(F_M - F_O)$	relative variable fluorescence at the J step
$V_I = (F_I - F_O)/(F_M - F_O)$	relative variable fluorescence at the I step
$M_0 \equiv 4(F_{270\mu s} - F_O)/(F_M - F_O)$	transient normalized on the maximal variable fluorescence F_V
$S_m \equiv Area/(F_M - F_O)$	normalized total complementary area above the O-J-I-P transient (reflecting multiple-turnover Q_A reduction events)
$N \equiv S_m/S_s = S_m \cdot M_0/V_J$	turnover number: number of Q_A reduction events between time 0 and t_{FM}
Quantum efficiencies or flux ratios	
$\varphi_{Po} = PHI(P_0) = TR_0/ABS = 1 - F_O/F_M$	maximum quantum yield for primary photochemistry
$\psi_{Eo} = PSI_0 = ET_0/TR_0 = (1 - V_J)$	probability that an electron moves further than Q_A^-
$\varphi_{Eo} = PHI(E_0) = ET_0/ABS = (1 - F_O/F_M)(1 - V_J)$	quantum yield for electron transport (ET)
$\gamma_{RC} = Chl_{RC}/Chl_{total} = RC/(ABS + RC)$	probability that a PSII Chl molecule functions as RC
Specific energy fluxes	
$ET_0/RC = M_0 \cdot (1/V_J) \cdot (1 - V_J)$	electron transport flux per RC (at t = 0)
Density of RCs	
$S_m/t_{FM} = [RC_{open}/(RC_{close} + RC_{open})]$ av	average fraction of open RCs of PSII in the time span between 0 to t_{FM}
$R_J = [\psi_{Eo(mock)} - \psi_{Eo(treatment)}]/\psi_{Eo(mock)}$	number of PSII RCs with Q_B-site filled by PSII inhibitor
Performance indexes	
$PI_{ABS} \equiv \frac{\gamma_{RC}}{1-\gamma_{RC}} \cdot \frac{\phi_{Po}}{1-\phi_{Po}} \cdot \frac{\psi_{Eo}}{1-\psi_{Eo}}$	performance index (potential) for energy conservation from photons absorbed by PSII to the reduction of intersystem electron acceptors

Subscript "0" (or "o" when written after another subscript) indicates that the parameter refers to the onset of illumination, when all RCs are assumed to be open.

3.5. Modeling of Four Mycotoxins in the Q_B Binding Site

The crystal structure information of the D1 protein of *C. reinhardtii* was obtained from the Protein Data Bank (https://rcsb.org, accessed on 17 January 2023, PDB code: 6KAC; the resolution: 2.70 Å). Its dimeric structure was optimized by CHARMm force field using Discovery Studio (version 2016, BIOVIA, San Diego, CA, USA). The structures of DCMU and the four mycotoxins as ligands were constructed using ChemDraw 18.0 (Cambridge Soft, MA, USA). The ligand structures were energetically minimized using the MM2 energy minimizations tool in Chem3D Pro 14.0 (Cambridge Soft, MA, USA). The possible binding site of ligands docking was set to the Q_B binding site in the D1 crystal structure of *C. reinhardtii* (PDB: 6KAC). The molecular docking was performed with CDocker in Discovery Studio. For the setting of the docking parameters, the Top Hits was set to 10, and the Pose Cluster Radius was set to 0.5 Å. We used the default values for the other parameters.

3.6. Statistical Analysis

One-way ANOVA was carried out, and means were separated by Duncan's LSD at 95% using SPSS Statistics 20.0 (IBM, CA, USA).

4. Conclusions

In conclusion, we showed that the mycotoxins fumagillin, mevastatin, radicicol, and wortmannin exhibit multiple negative effects on the photosynthetic process of *C. reinhardtii* cells. These mycotoxins disrupt PSII RCs by occupying the Q_B site, then block the electron transport flow from Q_A to Q_B, and finally inhibit photosynthetic activity. The four mycotoxins form a hydrogen bond with the Q_B site via the D1-Phe265 residue, which is different from classical PSII herbicides. The structures of these mycotoxins may provide ideas for the discovery of novel derivatives with stronger herbicide activity. However, the more precise binding conditions of the mycotoxins need to be further explored.

Author Contributions: S.C. designed the experiments. J.S., M.J., H.W., Z.L. and Y.C. carried out experiments. S.C., Y.G., H.W., J.S., R.J.S., H.M.K., S.Q. and X.Z. analyzed the data. J.S., M.J., H.W., Z.L. and Y.G. wrote the paper. S.C. revised the manuscript and prepared the final version. All authors contributed to and approved the final manuscript. All authors have read and agreed to the published version of the manuscript.

Funding: This work was supported by the Jiangsu Agriculture Science and Technology Innovation Fund (CX(21)3093), Fundamental Research Funds for the Central Universities (KYZ201530), and Foreign Expert Project (G2021145011L).

Institutional Review Board Statement: Not applicable.

Informed Consent Statement: Not applicable.

Data Availability Statement: Not applicable.

Acknowledgments: The authors thank editors and reviewers for their hard work and kind comments for this paper.

Conflicts of Interest: The authors declare no conflict of interest.

References

1. Bennett, J.W.; Klich, M. Mycotoxins. *Clin. Microbiol. Rev.* **2003**, *16*, 497–516. [CrossRef] [PubMed]
2. Wang, H.; Guo, Y.; Luo, Z.; Gao, L.; Li, R.; Zhang, Y.; Kalaji, H.M.; Qiang, S.; Chen, S. Recent advances in *Alternaria* phytotoxins: A review of their occurrence, structure, bioactivity and biosynthesis. *J. Fungi* **2022**, *8*, 168. [CrossRef]
3. Dayan, F.E.; Duke, S.O. Protoporphyrinogen oxidase-inhibiting herbicides. *Plant Physiol.* **2010**, *166*, 1090–1105. [CrossRef] [PubMed]
4. Guruceaga, X.; Perez-Cuesta, U.; Abad-Diaz de Cerio, A.; Gonzalez, O.; Alonso, R.M.; Hernando, F.L.; Ramirez-Garcia, A.; Rementeria, A. Fumagillin, a mycotoxin of *Aspergillus fumigatus*: Biosynthesis, biological activities, detection, and applications. *Toxins* **2020**, *12*, 7. [CrossRef] [PubMed]
5. Sin, N.; Meng, L.; Wang, M.; Wen, J.; Bornmann, W.; Crews, C. The anti-angiogenic agent fumagillin covalently binds and inhibits the methionine aminopeptidase, MetAP-2. *Proc. Natl. Acad. Sci. USA* **1997**, *94*, 6099–6103. [CrossRef]
6. van den Heever, J.P.; Thompson, T.S.; Curtis, J.M.; Ibrahim, A.; Pernal, S.F. Fumagillin: An overview of recent scientific advances and their significance for apiculture. *J. Agric. Food Chem.* **2014**, *63*, 2728–2737. [CrossRef] [PubMed]
7. Ross, S.; Giglione, C.; Pierre, M.; Espagne, C.; Meinnel, T. Functional and developmental impact of cytosolic protein N-terminal methionine excision in *Arabidopsis*. *Plant Physiol.* **2005**, *137*, 623–637. [CrossRef] [PubMed]
8. Endo, A.; Kuroda, M.; Tsujita, Y. ML-236A, ML-236B, and ML236C, new inhibitors of cholesterogenesis produced by *Penicillium citrinium*. *J. Antibiot.* **1976**, *29*, 1346–1348. [CrossRef]
9. Soto, G.; Stritzler, M.; Lisi, C.; Alleva, K.; Pagano, M.; Ardila, F.; Mozzicafreddo, M.; Cuccioloni, M.; Angeletti, M.; Ayub, N. Acetoacetyl-CoA thiolase regulates the mevalonate pathway during abiotic stress adaptation. *J. Exp. Bot.* **2011**, *62*, 5699–5711. [CrossRef]
10. Delmotte, P.; Delmotte-Plaquee, J. A new antifungal substance of fungal origin. *Nature* **1953**, *171*, 344. [CrossRef]
11. Bang, S.; Shim, S.H. Beta resorcylic acid lactones (RALs) from fungi: Chemistry, biology, and biosynthesis. *Arch. Pharm. Res.* **2020**, *43*, 1093–1113. [CrossRef]
12. Inoue, H.; Li, M.; Schnell, D.J. An essential role for chloroplast heat shock protein 90 (Hsp90C) in protein import into chloroplasts. *Proc. Natl. Acad. Sci. USA* **2013**, *110*, 3173–3178. [CrossRef] [PubMed]
13. Abbas, H.; Mirocha, C. Isolation and purification of a hemorrhagic factor (wortmannin) from *Fusarium oxysporum* (N17B). *Appl. Environ. Microbiol.* **1988**, *54*, 1268–1274. [CrossRef]
14. Matsuoka, K.; Bassham, D.; Raikhel, N.; Nakamura, K. Different sensitivity to wortmannin of two vacuolar sorting signals indicates the presence of distinct sorting machineries in tobacco cells. *J. Cell Biol.* **1995**, *130*, 1307–1318. [CrossRef]

15. Robinson, D.G.; Jiang, L.; Schumacher, K. The endosomal system of plants: Charting new and familiar territories. *Plant Physiol.* **2008**, *147*, 1482–1492. [CrossRef] [PubMed]
16. Workman, P.; Clarke, P.A.; Raynaud, F.I.; van Montfort, R.L.M. Drugging the PI3 kinome: From chemical tools to drugs in the clinic. *Cancer Res.* **2010**, *70*, 2146–2157. [CrossRef] [PubMed]
17. Wang, J.; Cai, Y.; Miao, Y.; Lam, S.; Jiang, L. Wortmannin induces homotypic fusion of plant prevacuolar compartments. *J. Exp. Bot.* **2009**, *60*, 3075–3083. [CrossRef]
18. Okazaki, K.; Miyagishima, S.; Wada, H. Phosphatidylinositol 4-Phosphate negatively regulates chloroplast division in *Arabidopsis*. *Plant Cell* **2015**, *27*, 663–674. [CrossRef]
19. Xiong, J.; Subramaniam, S.; Govindjee. Modeling of the D1/D2 proteins and cofactors of the photosystem II reaction center: Implications for herbicide and bicarbonate binding. *Protein Sci.* **1996**, *5*, 2054–2073. [CrossRef]
20. Fedtke, C.; Duke, S.O. Herbicides. In *Plant Toxicology*, 4th ed.; Hock, B., Elstner, E.F., Eds.; Marcel Dekker: New York, NY, USA, 2005; pp. 247–330.
21. Strasser, R.J.; Tsimilli-Michael, M.; Srivastava, A. Analysis of the chlorophyll a fluorescence transient. In *Chlorophyll a Fluorescence: A Signature of Photosynthesis*; Papageorgiou, G.C., Ed.; Springer: Dordrecht, The Netherlands, 2004; Volume 19, pp. 321–362.
22. Stirbet, A.; Govindjee. On the relation between the Kautsky effect (Chlorophyll *a* fluorescence induction) and photosystem II: Basics and applications of the OJIP fluorescence transient. *J. Photochem. Photobiol. B Biol.* **2011**, *104*, 236–257. [CrossRef]
23. Chen, L.S.; Li, P.; Cheng, L. Effects of high temperature coupled with high light on the balance between photooxidation and photoprotection in the sun-exposed peel of apple. *Planta* **2008**, *228*, 745–756. [CrossRef]
24. Tóth, S.Z.; Oukarroum, A.; Schansker, G. Probing the photosynthetic apparatus noninvasively in the laboratory of Reto Strasser in the countryside of Geneva between 2001 and 2009. *Photosynthetica* **2020**, *58*, 560–572. [CrossRef]
25. Lazar, D. The polyphasic chlorophyll *a* fluorescence rise measured under high intensity of exciting light. *Funct. Plant Biol.* **2006**, *33*, 9–30. [CrossRef] [PubMed]
26. Chen, S.; Xu, X.; Dai, X.; Yang, C.; Qiang, S. Identification of tenuazonic acid as a novel type of natural photosystem II inhibitor binding in Q_B-site of *Chlamydomonas reinhardtii*. *Biochim. Biophys. Acta* **2007**, *1767*, 306–318. [CrossRef] [PubMed]
27. Chen, S.; Strasser, R.J.; Qiang, S. In vivo assessment of effect of phytotoxin tenuazonic acid on PSII reaction centers. *Plant Physiol. Biochem.* **2014**, *84*, 10–21. [CrossRef]
28. Chen, S.; Zhou, F.; Yin, C.; Strasser, R.J.; Yang, C.; Qiang, S. Application of fast chlorophyll *a* fluorescence kinetics to probe action target of 3-acetyl-5-isopropyltetramic acid. *Environ. Exp. Bot.* **2011**, *71*, 269–279. [CrossRef]
29. Jiang, H.X.; Chen, L.S.; Zheng, J.G.; Han, S.; Tang, N.; Smith, B.R. Aluminum-induced effects on Photosystem II photochemistry in Citrus leaves assessed by the chlorophyll *a* fluorescence transient. *Tree Physiol.* **2008**, *28*, 1863–1871. [CrossRef]
30. Pinior, A.; Grunewaldt-Stocker, G.; von Alten, H.; Strasser, R.J. Mycorrhizal impact on drought stress tolerance of rose plants probed by chlorophyll *a* fluorescence, proline content and visual scoring. *Mycorrhiza* **2005**, *15*, 596–605. [CrossRef]
31. Srivastava, A.; Jüttner, F.; Strasser, R.J. Action of the allelochemical, fischerellin A, on photosystem II. *Biochim. Biophys. Acta* **1998**, *1364*, 326–336. [CrossRef] [PubMed]
32. Guo, Y.; Liu, W.; Wang, H.; Wang, X.; Qiang, S.; Kalaji, H.M.; Strasser, R.J.; Chen, S. Action mode of the mycotoxin patulin as a novel natural photosystem II inhibitor. *J. Agric. Food Chem.* **2021**, *69*, 7313–7323. [CrossRef] [PubMed]
33. Jacob, J.; Lawlor, D.W. In vivo photosynthetic electron transport does not limit photosynthetic capacity in phosphate-deficient sunflower and maize leaves. *Plant Cell Environ.* **1993**, *16*, 785–795. [CrossRef]
34. Lin, Z.H.; Chen, L.S.; Chen, R.B.; Zhang, F.Z.; Jiang, H.X.; Tang, N. CO_2 assimilation, ribulose-1,5-bisphosphate carboxylase/oxygenase, carbohydrates and photosynthetic electron transport probed by the JIP-test, of tea leaves in response to phosphorus supply. *BMC Plant Biol.* **2009**, *9*, 43. [CrossRef] [PubMed]
35. Wu, D.H.; Yang, C.Y.; Zhang, X.; Hou, X.P.; Zhang, S.Q.; Dai, X.Z.; Zhang, X.H.; Igarashi, Y.; Luo, F. Algicidal effect of tryptoline against *Microcystis aeruginosa*: Excess reactive oxygen species production mediated by photosynthesis. *Sci. Total Environ.* **2022**, *806*, 150719. [CrossRef]
36. Trebst, A. The three-dimensional structure of the herbicide binding niche on the reaction center polypeptides of photosystem II. *Z. Naturforsch.* **1987**, *42*, 742–750. [CrossRef]
37. Oettmeier, W. Herbicide resistance and super sensitivity in photosystem II. *Cell Mol. Life Sci.* **1999**, *55*, 1255–1277. [CrossRef]
38. Battaglino, B.; Grinzato, A.; Pagliano, C. Binding properties of photosynthetic herbicides with the Q_B Site of the D1 protein in plant photosystem II: A combined functional and molecular docking study. *Plants* **2021**, *10*, 1051. [CrossRef]
39. Lancaster, C.R.D.; Michel, H. Refined crystal structures of reaction centres from *Rhodopseudomonas viridis* in complexes with the herbicide atrazine and two chiral atrazine derivatives also lead to a new model of the bound carotenoid. *J. Mol. Biol.* **1999**, *286*, 883–898. [CrossRef] [PubMed]
40. Erickson, J.M.; Pfister, K.; Rahire, M.; Togasaki, R.K.; Mets, L.; Rochaix, J.D. Molecular and biophysical analysis of herbicide-resistant mutants of *Chlamydomonas reinhardtii* structure-function relationship of the photosystem II D1 polypeptide. *Plant Cell* **1989**, *1*, 361–371.
41. Murphy, B.P.; Tranel, P.J. Target-site mutations conferring herbicide resistance. *Plants* **2019**, *8*, 382. [CrossRef]

42. Wang, H.; Yao, Q.; Guo, Y.; Zhang, Q.; Wang, Z.; Strasser, R.J.; Valverde, B.E.; Chen, S.; Qiang, S.; Kalaji, H.M. Structure-based ligand design and discovery of novel tenuazonic acid derivatives with high herbicidal activity. *J. Adv. Res.* **2022**, *40*, 29–44. [CrossRef]
43. Guo, Y.; Cheng, J.; Lu, Y.; Wang, H.; Gao, Y.; Shi, J.; Yin, C.; Wang, X.; Chen, S.; Strasser, R.J.; et al. Novel action targets of natural product gliotoxin in photosynthetic apparatus. *Front. Plant Sci.* **2020**, *10*, 1688. [CrossRef] [PubMed]